# Extended Coulomb approximation for multichannel-quantum-defect-theory computations of dipole moments: Method of calculation and application to $H_2$

A. Matzkin and Ch. Jungen

*Laboratoire Aimé-Cotton, Centre National de la Recherche Scientifique, Université de Paris–Sud, 91405 Orsay, France*

S. C. Ross

*Department of Physics, University of New Brunswick, Fredericton, New Brunswick, Canada E3B 5A3*

A method for calculating dipole transition moments in effective one-electron systems when some channels are closed is investigated within the framework of multichannel quantum-defect theory (MQDT). A treatment of the energy dependence is also given. This method is useful when electronic channel interactions occur and MQDT is combined with frame transformations. Our calculations are made in the Coulomb approximation and include provisions for core transitions. They are tested by comparing transitions between bound states of molecular hydrogen with *ab initio* computations. [S1050-2947(98)03912-2]

PACS number(s): 32.70.Cs, 31.50.+w, 32.80.Fb, 34.60.+z

## I. INTRODUCTION

Dipole transition moments are among the main physical quantities associated with the theoretical calculations of photoionization spectra. As is known, in a diatomic molecule the transition from a low-energy state for which the wave function is near the core to a higher Rydberg or continuum wave function can be understood in terms of a frame transformation: Before excitation the electron is adequately described in a short-range formulation [Hund's case (a) or (c)], while once excited, it should be described in the laboratory frame [Hund's case (d) or (e)]. The frame transformation elements were extensively studied in a recent article by Jungen and Raseev (JR) [1], wherein readily usable expressions are given for the angular factors involved in the dipole transition moments. In the present paper we complete the work of JR by describing a method for calculating the radial part of dipole moments and their energy dependence.

The difficulty here is that unless the wave function of the outer electron in effective one-electron systems is known from quantum chemical or *R*-matrix calculations, close-range dipole moments smooth in energy cannot be defined in a straightforward manner: Within the framework of collision theories containing closed channels, such as multichannel quantum-defect theory (MQDT), divergent expressions appear in the transition integrals between closed (bound electron) channels. These exponentially divergent expressions are of mathematical nature, unlike the case of free-free transitions where the numerical divergences are eliminated by using the accelerator form of the dipole operator [2]. Our method is particularly appropriate in cases where the outer electron takes part in an electronic channel interaction and has a comparable energy before and after the transition. The MQDT analysis of $H_2$ carried on by Ross and Jungen [3,4] is an example of such a situation. Our approach can be viewed as an extension of the Coulomb approximation to the electronic multichannel case where transitions can affect the core state as well as the Rydberg electron. The dipole moment between two states is calculated by considering the transition elements between initial and final channels [5], thus avoiding recourse to state-to-state calculations.

In Sec. II we give a formulation for the radial part of dipole transitions in a diatomic molecule within the MQDT framework. Various ways of dealing with the energy dependence will be examined. In Sec. III we apply our formulation to the computation of dipole moments in molecular hydrogen in the Coulomb approximation. In Sec. IV electronic dipole transition moments are obtained and compared with state-to-state *ab initio* calculations [6,7]. We also give examples of the energy dependence of the dipole moments for transitions to high Rydberg or continuum states. Finally, in Sec. V the validity of the Coulomb approximation is discussed and a specific treatment for large internuclear distances is considered.

## II. DIPOLE MOMENT FORMULATIONS

### A. Molecular wave functions

A highly excited molecule can autoionize and eject an electron. It is represented by a standing wave [see Eq. (17) of JR]

$$\psi_\rho = \sum_{I=1}^{N} \sum_{I'=1}^{N} \Phi_I [f_I(r) C_{II'} - g_I(r) S_{II'}] B_{I'}^\rho, \qquad (1)$$

whose combinations account for the outgoing electron. $\Phi_I$ denotes the wave function of the core in the rovibronic state $I^+$, as well as the electron's angular momentum $l_i$ and spin: $I = \{I^+, l_i, j_i\}$; $f_I(r)$ and $g_I(r)$ are the regular and irregular radial functions of the outer electron (here Coulomb functions, as we will suppose a pure Coulomb field outside the core). MQDT does not give the wave function inside the core and so Eq. (1) is valid only for $r$ larger than the core radius $r_0$. $\mathbf{K} = \mathbf{S}\mathbf{C}^{-1}$ is the reaction matrix explicitly containing the closed channels (thus of dimension $N \times N$, with $N = N_o + N_c$ being the sum of open and closed channels). The physical reaction matrix $\mathbf{K}(E)$ of dimensions $N_o \times N_o$ is related to the scattering matrix $\mathbf{S}(E)$ by $\mathbf{K}(E) = -i[\mathbf{S}(E) - I][\mathbf{S}(E) + I]^{-1}$. The eigenvalues of $\mathbf{K}(E)$ and the channel coeffi-

cients $B_{I'}^{\rho}$ are determined in the typical MQDT diagonalization procedure [8]. The label $\rho$ denotes the eigenstates of the open-channel interaction.

For $r$ values near the core, the wave function is formulated in a manner appropriate at short range [Hund's case (a), the molecular frame],

$$\psi_{\rho} \approx \sum_{i=1}^{N} \sum_{i'=1}^{N} X_i [f_{l_i}(r) C_{ii'} - g_{l_i}(r) S_{ii'}] A_{i'}^{\rho}, \qquad (2)$$

equivalent to Eq. (23) of JR. Here $i = \{S_i, \Lambda_i, \Omega_i, i^+, l_i, \lambda_i\}$, which is similar to the label $\beta$ used by JR, although in the present work the set of indices $i$ and $I$ will essentially be used to distinguish electronic ($i$) from rovibronic ($I$) quantities. The dependence on rotation and vibration is now included in the factors $X_i$, as will be specified in Sec. III below. The $X_i$ are related to the $\Phi_I$ by transforming Eq. (1) to the molecular frame. $C_{II'}$ and $S_{II'}$ are deduced from $C_{ii'}$ and $S_{ii'}$ via a rovibronic frame transformation matrix $\mathbf{U}$,

$$C_{II'} = \sum_{i,i'} U_{Ii} C_{ii'} U_{i'I'}^{\mathrm{tr}}. \qquad (3)$$

The same is true for the coefficients

$$B_{I'}^{\rho} = \sum_{i'} U_{I'i'} A_{i'}^{\rho}. \qquad (4)$$

$C_{ii'}$ and $S_{ii'}$ are assumed to be diagonal in $S$, $\Lambda$, and $\Omega$, which are good quantum numbers in Hund's case (a).

### B. Radial behavior and transition moments

The dipole transition moment between $\psi_{\rho}$ and a low-energy state $\psi_0$ is given by

$$D_0^{\rho} = \langle \psi_0 | \mathbf{D} | \psi_{\rho} \rangle. \qquad (5)$$

For the sake of simplicity, we will take the low-energy molecular wave function, accordingly stated in Hund's case (a), as a product of a single core function and an electron channel

$$\psi_0 = X_{i''} [f_{i''}(r) \cos(\pi \mu_{i''}) - g_{i''}(r) \sin(\pi \mu_{i''})]. \qquad (6)$$

Here the $\mathbf{C}$ and $\mathbf{S}$ matrices are expressed in terms of the single-channel quantum defect $\mu_{i''}$ and we have $D_0^{\rho} = D_{i''}^{\rho}$. Of course $\psi_0$ could as well include a sum of several channels and core states; this generalization is straightforward.

Since the double sum in Eq. (2) includes closed channels, the expressions have to be used with particular attention. As is known, for negative (Rydberg electron) energies the functions $f$ and $g$ both diverge at $r \to \infty$. This strong, usually exponential, divergence appears for $r$ values beyond the classical turning point $r_t$, while $f$ and $g$ are well behaved for $r \leqslant r_t$. Obviously, the turning point depends on the outer electron's energy $\epsilon_i$, given by

$$\epsilon_i = E - E_i^+, \qquad (7)$$

with $E_i^+$ being the energy of the ion in the $i$ state and $E$ the total energy of the molecule.

Thus, for each closed ($Q$) channel $i$, we must have in the limit $r \to \infty$

$$\sum_{i'} [f_{l_i}(r) C_{ii'} - g_{l_i}(r) S_{ii'}] A_{i'}^{\rho} \to 0, \quad i \in Q. \qquad (8)$$

Although this expression is well behaved, each term in square brackets taken individually will diverge. As a consequence, if Eq. (2) is expressed as

$$\psi_{\rho} = \sum_{i'=1}^{N} A_{i'}^{\rho} \psi_{i'}, \qquad (9)$$

with $\psi_{i'}$ given by

$$\psi_{i'} = \sum_{i=1}^{N} X_i [f_{l_i}(r) C_{ii'} - g_{l_i}(r) S_{ii'}], \qquad (10)$$

then each term diverges at large $r$, as soon as $r \geqslant r_t(\epsilon_i)$.

This affects the corresponding expressions of the dipolar moments. If we partition the dipole transition moment as

$$D_{i''}^{\rho} = \sum_{i'} D_{i''}^{i'} A_{i'}^{\rho}, \qquad (11)$$

with

$$D_{i''}^{i'} = \langle \psi_0 | \mathbf{D} | \psi_{i'} \rangle, \qquad (12)$$

this last expression formally diverges. However, $D_{i''}^{i'}$ can nevertheless be defined if (a) the lower state radial function $f_{i''}(r) \cos(\pi \mu_{i''}) - g_{i''}(r) \sin(\pi \mu_{i''})$ goes to 0 for $r$ greater than the classical turning point $r_t(\epsilon_{i'})$ of $\psi_{i'}$, thereby annihilating the divergence of $\psi_{i'}$, or (b) $C_{ii'}$ and $S_{ii'}$ are diagonal and thus Eq. (8) reduces to a single convergent term.

Fortunately in previous calculations [9–11], these conditions were fulfilled. In all other situations, Eqs. (11) and (12) and the expression (21b) of JR are, strictly speaking, divergent. However, we will see below how these formally infinite quantities can be parametrized.

In general, Eq. (5) has to be expressed by making the physical quantization condition that has to be made for each electron in state $i$ appear explicitly regardless of what the nonperturbed channel before the collision was. Equation (2) can be rearranged as

$$\psi_{\rho} \approx \sum_{i=1}^{N} X_i \left[ f_{l_i}(r) \sum_{i'=1}^{N} A_{i'}^{\rho} C_{ii'} - g_{l_i}(r) \sum_{i'=1}^{N} \bar{A}_{i'}^{\rho} S_{ii'} \right]$$

$$\equiv \sum_{i=1}^{N} X_i [f_{l_i}(r) \cos \pi \bar{\mu}_i^{\rho} - g_{l_i}(r) \sin \pi \bar{\mu}_i^{\rho}] \bar{A}_i^{\rho}, \qquad (13)$$

with $\bar{A}_i^{\rho}$ and $\bar{\mu}_i^{\rho}$ given by

$$\sum_{i'=1}^{N} A_{i'}^{\rho} C_{ii'} \equiv \bar{A}_i^{\rho} \cos \pi \bar{\mu}_i^{\rho},$$

$$\sum_{i'=1}^{N} A_{i'}^{\rho} S_{ii'} \equiv \bar{A}_i^{\rho} \sin \pi \bar{\mu}_i^{\rho}. \qquad (14)$$

The $\bar{\mu}_i^{\rho}$ are known as *effective* quantum defects and the $\bar{A}_i^{\rho}$ are the effective channel coefficients. By matching boundary conditions for closed ($Q$) and open ($P$) channels, it can be established that

$$\bar{\mu}_i^{\rho} = n - \nu_i, \quad i \in Q$$
$$\bar{\mu}_i^{\rho} = \tau_\rho, \quad i \in P, \qquad (15)$$

where $n$ is an integer, $\nu_i = (-\epsilon_i)^{-1/2}$ (Rydberg units will be used throughout), and $\tan \pi \tau_\rho$ are the eigenvalues of the physical reaction matrix $\mathbf{K}(E)$. Accordingly, the dipole transition moment $D_{i''}^{\rho}$ may be expanded as

$$D_{i''}^{\rho} = \sum_{i'} \bar{D}_{i''}^{i'} \bar{A}_{i'}^{\rho}, \qquad (16)$$

with

$$\bar{D}_{i''}^{i'} = \langle \psi_0 | \mathbf{D} | [f_{l_{i'}}(r) \cos \pi \bar{\mu}_{i'}^{\rho} - g_{l_{i'}}(r) \sin \pi \bar{\mu}_{i'}^{\rho}] | X_{i'} \rangle. \qquad (17)$$

This expression is well defined in all circumstances. Note, however, that it is expected to vary substantially with the energy since the boundedness of the closed channels has been included in the $\bar{D}_{i''}^{i'}$. On the other hand, when defined, the $D_{i''}^{i'}$ involve only short-range interactions (i.e., without taking account of the large-$r$ behavior) and are expected to be smoother in energy.

### C. Energy dependence

The main problem arising in practical computations of transitions to high-energy Rydberg states comes from the strong energy dependence of the $\bar{D}_{i''}^{i'}$ of Eq. (17). Since the dipole operator in our effective one-electron system is a sum of the outer-electron dipole and the core transition dipole operators (see Sec. III B below), the energy dependence, as well as the divergences, is confined to the radial integrals between the initial state and the manifold of final states. The strong energy dependence of the radial integrals can be circumvented in either of two ways: (i) directly, by factoring the energy dependence of the radial integral in $\bar{D}_{i''}^{i'}$ into a smooth part related to short-range effects and a strongly varying part coming from imposing boundary conditions at large $r$, or (ii) by parametrizing the formally divergent radial parts of $D_{i''}^{i'}$ of Eq. (12) in such a way that the total standing-wave transition moment (5) is recovered when calculated with the formally divergent equation (11). Each of these approaches is discussed in turn below.

#### 1. Factoring the energy dependence of the $\bar{D}_{i''}^{i'}$

For $\epsilon_i < 0$ we write the effective channel radial function, in large square brackets in Eq. (13), as

$$\phi_i(\epsilon_i, r) = f_i(r) \cos \pi \bar{\mu}_i^{\rho} - g_i(r) \sin \pi \bar{\mu}_i^{\rho} \qquad (18)$$

and let $\phi_0(\epsilon_{i''}, r)$ be the lower state radial function. Simple trigonometry and Eq. (15) yield

$$\langle \phi_0 | r^q | \phi_i(\epsilon_i) \rangle = \cos \pi n \{ \cos \pi(\nu_i - \varkappa) d_1(\epsilon_i) - \sin \pi(\nu_i - \varkappa) d_2(\epsilon_i) \}. \qquad (19)$$

This is the type of radial integral that appears in the expression of $\bar{D}_{i''}^{i'}$ [Eq. (17)], with $q = 0$ or 1. $d_1(\epsilon_i)$ and $d_2(\epsilon_i)$ are defined by

$$d_1(\epsilon_i) = \langle \phi_0 | r^q | f_i(\epsilon_i) \cos \pi \varkappa + g_i(\epsilon_i) \sin \pi \varkappa \rangle \qquad (20)$$

and

$$d_2(\epsilon_i) = \langle \phi_0 | r^q | f_i(\epsilon_i) \cos \pi(\varkappa - \tfrac{1}{2}) + g_i(\epsilon_i) \sin \pi(\varkappa - \tfrac{1}{2}) \rangle. \qquad (21)$$

Here $n$ is an integer according to Eq. (15) and $\varkappa$ is an arbitrary parameter allowing for this radial basis change. For a given value of $\varkappa$, $d_1(\epsilon_i)$ is strictly defined only for $\nu_i = \varkappa + n'$, while $d_2(\epsilon_i)$ is defined if $\nu_i = \varkappa + n' + \tfrac{1}{2}$, where $n'$ is an integer. For those values, $d_1(\epsilon_i)$ and $d_2(\epsilon_i)$ are smoothly dependent on energy.

Since the left-hand side of Eq. (19) is defined for all $\epsilon_i$, so is the right-hand side. For a fixed value of $\varkappa$ we evaluate $d_1(\epsilon_i)$ and $d_2(\epsilon_i)$ at the appropriate values of $\nu_i$ and then interpolate between them. Henceforth $d_1(\epsilon_i)$ and $d_2(\epsilon_i)$ are defined at every energy. We have thus parametrized the energy dependence of the radial integral and thus of the $\bar{D}_{i''}^{i'}$ into smooth parts and strong oscillating parts (cosine and sine factors) that take into account the boundary conditions. This will be illustrated in Sec. IV C.

For $\epsilon_i > 0$ the same technique can be used by replacing $\bar{\mu}_i^{\rho}$ by $\tau_\rho$ according to Eq. (15) and setting the proper signs. We remark that we have implicitly used phase-shifted radial pairs; this has been repeatedly employed in MQDT in relation to closed-channel connected effects, such as resonant structures (see, e.g., [12,13]).

#### 2. Parametrization of the $D_{i''}^{i'}$

By combining Eqs. (12) and (9) [or, equivalently, by examining the expressions in curly brackets in Eq. (32) below] we see that each term of the sum making up $D_{i''}^{i'}$ has a radial (divergent) part given by

$$d_{i''}^{i}(\epsilon_i) = \langle \phi_0 | r^q | f_i C_{ii'} - g_i S_{ii'} \rangle. \qquad (22)$$

From Eqs. (20) and (21) we extract

$$d_{f_i}(\epsilon_i) \equiv \langle \phi_0 | r^q | f_i(\epsilon_i) \rangle = \cos(\pi \varkappa) d_1(\epsilon_i) + \sin(\pi \varkappa) d_2(\epsilon_i), \qquad (23)$$

$$d_{g_i}(\epsilon_i) \equiv \langle \phi_0 | r^q | g_i(\epsilon_i) \rangle = \sin(\pi \varkappa) d_1(\epsilon_i) - \cos(\pi \varkappa) d_2(\epsilon_i), \qquad (24)$$

where $d_1(\epsilon_i)$ and $d_2(\epsilon_i)$ represent the smooth interpolated functions. Despite the fact that $\langle \phi_0 | r^q | f_i(\epsilon_i) \rangle$ converges only for given values of negative $\epsilon_i$ [namely, when the effective quantum number $\nu_i = (-\epsilon_i)^{-1/2}$ is a whole number],

Eq. (23) now gives a parametrization of this expression. The meaning of this parametrization is clear: By leaving aside the actual long-range boundary condition, we get smoothly varying $d_{f_i}$ and $d_{g_i}$ and thus transition integrals

$$d_{i''}^i(\epsilon_i) = d_{f_i}(\epsilon_i)C_{ii'} - d_{g_i}(\epsilon_i)S_{ii'}, \tag{25}$$

which vary smoothly with the energy. These quantities are the parametrized radial factors of the $D_{i''}^{i'}$ defined by Eq. (12) and have been constructed so that for the physical energies the correct transition integral, defined by the left-hand side of Eq. (19), is recovered. In other words, with this parametrization of the radial factors Eq. (11) gives the same result as the formally correct formulation (17). Its main advantage lies in that smooth $D_{i''}^{i'}$ reflecting short-range interaction phenomena are obtained. These $D_{i''}^{i'}$ are then of easier use in practical computations, for example, in the context of frame transformations with electronic interactions (see Sec. IV C).

## III. ROVIBRONIC WAVE FUNCTIONS AND DIPOLE MOMENTS IN $H_2$

### A. Frame transformation

$H_2$ has been the prototype for applications of MQDT to molecular problems. Since 1994, electronic quantum defects have been available for different gerade and ungerade symmetries of the molecule [3].

At large $r$ the electron is uncoupled [i.e., Hund's case (d), given that spin-orbit coupling is negligible]. By setting $I = i^+ v_i^+ N_i^+$ and $\Phi_I = |i^+ v_i^+ N_i^+\rangle$, Eq. (1) can be written as in Ref. [3]:

$$\psi_\rho = \sum_{i,v_i^+,N_i^+} \sum_{j,v_j^+,N_j^+} |iv_i^+N_i^+\rangle B_{jv_j^+N_j^+}^\rho$$

$$\times [f_{l_iv_i^+N_i^+}(r)C_{iv_i^+N_i^+,jv_j^+N_j^+}$$

$$- g_{l_iv_i^+N_i^+}(r)S_{iv_i^+N_i^+,jv_j^+N_j^+}], \tag{26}$$

where $i$ refers to the electronic core state and the orbital angular momentum of the outer electron quantized in the laboratory frame [in Eq. (26)] or in the molecular frame [in Eq. (27)] and $v_i^+N_i^+$ are the vibrational and rotational numbers of the $H_2^+$ core. $f$ and $g$ are Coulomb functions taken at the energy $\epsilon_{iv_i^+N_i^+} = E - E_{iv_i^+N_i^+}^+$ of the Rydberg electron, $E$ being the energy of the molecule and $E^+$ the core energy.

However, near the core the wave function is written as a Born-Oppenheimer (BO) product [3]

$$\psi_\rho \approx \sum_{i,j,v,\Lambda} A_{jv\Lambda}^\rho |i(R)\rangle[f_i(r)C_{ij}^\Lambda(R) - g_i(r)S_{ij}^\Lambda(R)]|v\Lambda\rangle, \tag{27}$$

with

$$A_{jv\Lambda}^\rho = \sum_{j,v_j^+,N_j^+} B_{jv_j^+N_j^+}^\rho \langle\Lambda|N_j^+\rangle\langle v|v_j^+\rangle \tag{28}$$

and

$$C_{iv_i^+N_i^+jv_j^+N_j^+} = \sum_\Lambda \sum_{v,v'} \langle iv_i^+N_i^+|i\Lambda v\rangle$$

$$\times \langle i\Lambda v|C_{ij}^\Lambda|j\Lambda v'\rangle\langle j\Lambda v'|jv_j^+N_j^+\rangle$$

$$= \sum_\Lambda \int dR\langle iv_i^+N_i^+|iR\Lambda\rangle C_{ij}^\Lambda(R)$$

$$\times \langle jR\Lambda|jv_j^+N_j^+\rangle, \tag{29}$$

and similarly for $S_{iv_i^+N_i^+jv_j^+N_j^+}$. Equation (28) is analogous to Eq. (4) (actually to its inverse), while Eq. (29) is just Eq. (3); we get the second line of Eq. (29) by using the closure relation for the molecular vibrational functions. Notice that the frame transformation represented by Eq. (29) involves, in addition to the rotational part, the internuclear coordinate $R$. The total reaction matrix in Hund's case (d), $\mathbf{K} = \mathbf{SC}^{-1}$, is thus related to the electronic $R$-dependent reaction matrices for each BO symmetry, $\mathbf{K}^\Lambda(R) = \mathbf{S}^\Lambda(R)[\mathbf{C}^\Lambda(R)]^{-1}$, that is, to the electronic quantum defects $\mu_{ij}^\Lambda(R) \equiv \pi^{-1}\arctan K_{ij}^\Lambda(R)$ (for more details, refer to [4]).

Once the frame transformation matrices are known, the problem of calculating the dipole transition moment between $\psi_\rho$ and a lower state is reduced to the calculation of the purely electronic $R$-dependent dipole moments

$$D_{i''}^\Lambda(R) = \sum_{i,j} A_{jv\Lambda}^\rho\langle i''|\langle f_{i''}\cos \pi\mu_{i''}^{\Lambda_0}(R)$$

$$- g_{i''}\sin \pi\mu_{i''}^{\Lambda_0}(R)|\mathbf{D}|f_iC_{ij}^\Lambda(R) - g_iS_{ij}^\Lambda(R)\rangle|i\rangle \tag{30}$$

where we have taken the lower-state wave function of Eq. (6) as a simple BO product

$$\psi_0 = |i''\rangle[f_{i''}(r)\cos \pi\mu_{i''}^{\Lambda_0}(R)$$

$$- g_{i''}(r)\sin \pi\mu_{i''}^{\Lambda_0}(R)]|\Lambda_0\rangle|v_0\rangle. \tag{31}$$

We have already pointed out that within MQDT, the wave function inside the core is not known [mathematically the irregular function $g(r)$ diverges when $r \to 0$]. Therefore, in the calculations of the dipole moments, we set a cutoff radius in the radial integrals as $r \to 0$. The validity of this procedure, known as the Coulomb approximation, will be discussed in Sec. V A.

### B. Core- and outer-electron transitions

The dipole operator can be taken as $\mathbf{D} = \mathbf{r} + \mathbf{r}_c$, where $\mathbf{r}$ and $\mathbf{r}_c$ are the outer and core electron position operators expressed in the molecular frame. Writing $|i\rangle$ explicitly in terms of the core state and the outer electron's angular momentum numbers $|i\rangle = |i^+\rangle|l_i\lambda_i\rangle$, Eq. (30) is accordingly set as an independent sum of the outer and inner electrons' transitions

$$D_{i''}^{\Lambda}(m) = \sum_{i,j} A_{jv\Lambda}^{\rho}\{\langle f_{i''}\cos \ \pi\mu_{i''}^{\Lambda 0}(R)$$

$$- g_{i''}\sin \ \pi\mu_{i''}^{\Lambda 0}(R)|r|f_i C_{ij}^{\Lambda}(R) - g_i S_{ij}^{\Lambda}(R)\rangle$$

$$\times \langle l_{i''}\lambda_{i''}|\mathbf{Y}_{1m}|l_i\lambda_i\rangle\langle i''^+|i^+\rangle\}$$

$$+ \sum_{i,j} A_{jv\Lambda}^{\rho}\{\langle f_{i''}\cos \ \pi\mu_{i''}^{\Lambda 0}(R)$$

$$- g_{i''}\sin \ \pi\mu_{i''}^{\Lambda 0}(R)|f_i C_{ij}^{\Lambda}(R) - g_i S_{ij}^{\Lambda}(R)\rangle$$

$$\times \langle l_{i''}\lambda_{i''}|l_i\lambda_i\rangle\langle i''^+|r_c\mathbf{Y}_{1m}|i^+\rangle\}. \tag{32}$$

The term in the first set of curly brackets is equivalent to Eq. (29a) of JR, while that in the second is their Eq. (29b). However, we have observed that unless condition (a) or (b) of Sec. II B is fulfilled, the expressions in curly brackets in Eq. (32) are not well defined because the radial part diverges for bound states. Since the electronic states in $H_2$ are generally represented by several interacting electronic channels with ground and excited core states, the transition computations require the use of the effective channel formulation of Eq. (16).

## IV. RESULTS

### A. Details of calculations

The dipole moments of Eq. (32) are formulated following Eq. (16), with energy-normalized radial functions; the quantum defects were taken from Ref. [3]. The whole wave function may be renormalized to unity for comparisons with *ab initio* calculations.

Since the wave function inside the core is not known, our calculations rely on the Coulomb approximation, introduced a long time ago by Bates and Damgaard [14]. They had observed that the dipole moments in systems with one effective outer electron subjected to a long-range Coulomb field were insensitive to the wave function inside the core. It is thus possible to neglect the interval between 0 and a cutoff radius $r_c$ in the transition integrals. It seems reasonable to choose $r_c \approx r_0$, $r_0$ being the core radius, even though in previous works the cutoff radius was often set inside the core so as to minimize the variation of the length form of the dipole matrix element. Since core transitions are also taken into account by the second sum in Eq. (32), the same cutoff radius was used in the overlap integrals. We have generally chosen $r_c \approx 2$ a.u. and checked the stability of the transition integrals. The validity of the Coulomb approximation will be discussed below. The electronic transition moments of the $H_2^+$ ion were taken from Ref. [15].

The parameter $\varkappa$ introduced in Eq. (19) is arbitrary to the extent that the numerical (e.g., quadratic) functions $d_1(\epsilon_i)$ and $d_2(\epsilon_i)$ are interpolated from sufficient values (i.e., the energy interval in terms of the effective quantum number is large enough). When this is not the case (typically when the Rydberg electron's energy is very low over the energy interval considered) the value of $\varkappa$ has to be chosen judiciously, so that $d_1(\epsilon_i)$ and $d_2(\epsilon_i)$ in Eq. (19) can easily be interpolated over the energy range with the (fixed) chosen $\varkappa$.
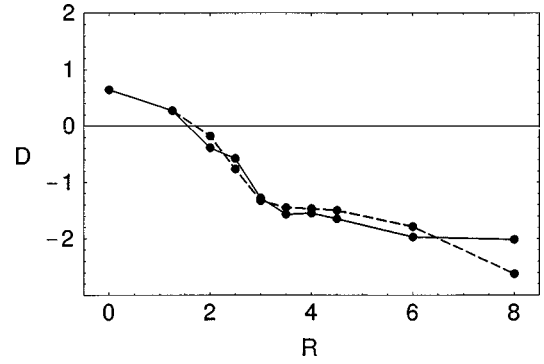


FIG. 1. $B$-$H\bar{H}$ electronic dipole transition moment $D$ (in units of $a_0$) as a function of the internuclear distance $R$: our results (solid line) and *ab initio* computations of Ref. [6] (dashed line).

### B. Examples of bound-bound singlet electronic transitions

#### 1. $B$ $^1\Sigma_u^+$ -$H\bar{H}$ $^1\Sigma_g^+$ transitions

The $B$ state is represented by a single channel, with a $(1s\sigma_g)$ ground core state and an $\epsilon p\sigma_u$ outer electron, while $\Sigma_g^+$ states are represented by three interacting channels: The $s$ channel $(1s\sigma_g)(\epsilon s\sigma_g)$, the $d$ channel $(1s\sigma_g)(\epsilon d\sigma_g)$, and the excited core $p$ channel $(2p\sigma_u)(\epsilon p\sigma_u)$. For the $B$-$H\bar{H}$ transition, as well as for transitions from $B$ to higher $\Sigma_g$ states, condition (a) of Sec. II is satisfied only for the $s$ and $d$ channels because at intermediate $R$ values the excited core keeps the outer $p$ electron's energy very low.

In Fig. 1 we compare our results (solid line) to those obtained in the *ab initio* computations of Ref. [6] (dashed line). For small $R$ values the $H\bar{H}$ state is mainly represented by the $s$ channel, so the dipole moment mainly involves an outer electron $p \rightarrow s$ transition. For $2.5 < R < 4.5$ nondiagonal quantum defects represent the interaction zone and the mixed nature of the $H\bar{H}$ state gives rise to $p \rightarrow s$ and $p \rightarrow d$ outer-electron transitions as well as $1s\sigma_g \rightarrow 2p\sigma_u$ core transitions. The agreement with the *ab initio* calculations is good, except for large internuclear distances ($R > 6$), where it is well known that the MQDT electronic wave function suffers from severe limitations (see Sec. V B).

#### 2. $C$ $^1\Pi_u$ -$I$ $^1\Pi_g$ and $C$ $^1\Pi_u$ -$R$ $^1\Pi_g$ transitions

The singlet $C$ state is represented by the channel $(1s\sigma_g)(\epsilon p\pi_u)$, while $\Pi_g$ states are combinations of $(1s\sigma_g)(\epsilon d\pi_g)$ and $(2p\sigma_u)(\epsilon p\pi_u)$ channels [16]. In Fig. 2 we compare our values to the *ab initio* calculations of Wolniewicz [7]. The $I$ and $R$ states are both represented by the sole $d$ channel at small $R$, while strong interactions prevail for $3.5 < R < 4.5$, thus giving rise to both $p \rightarrow d$ outer-electron and $1s\sigma_g \rightarrow 2p\sigma_u$ core transitions. For $R > 6$ the $d$ channel accounts for the $R$ state (and the dipole moment is given by a $p \rightarrow d$ transition), while the $I$ state is represented by the $p$ channel; this gives rise to an unphysical core transition, which must be corrected by following the prescriptions of Sec. V B. The result of doing so is represented by the short-dashed line in Fig. 2.

### C. Illustration of the energy dependence

As stated, we are interested in transitions towards high Rydberg or autoionizing states of $H_2$, where the energy de-
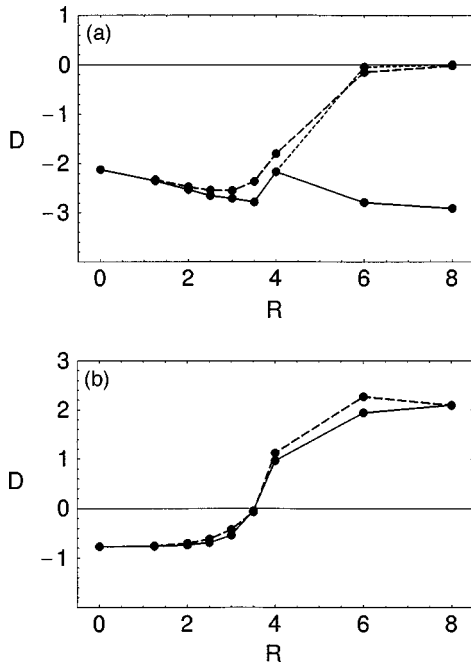
FIG. 2. Electronic dipole moment $D$ (in units of $a_0$) as a function of the internuclear distance $R$ for (a) $C$-$I$ and (b) $C$-$R$ transitions: our results (solid line) and *ab initio* computations of Ref. [7] (dashed line). The short-dashed line in (a) follows from the large internuclear distance treatment of Sec. V.

pendence of the channel transition moments is needed. Following the treatment of the energy dependence of the transition moments discussed in Sec. II, we consider below specific examples of transitions between a lower state and higher-energy channels in molecular hydrogen.

### 1. Effective electronic transition moment

Let us consider the specific example of the effective electronic transition moment from the $C$ state to the $d$ channel of the $\Sigma_g^+$ symmetry for $R=3$, denoted $\bar{D}_C^d(R=3)$. $\bar{D}_C^d(R=3)$ calculated using energy-normalized wave functions is plotted in Fig. 3 as a function of the effective quantum number $\nu$, where $\nu=(-\epsilon)^{-1/2}$ and $\epsilon$ is related to the molecular energy by
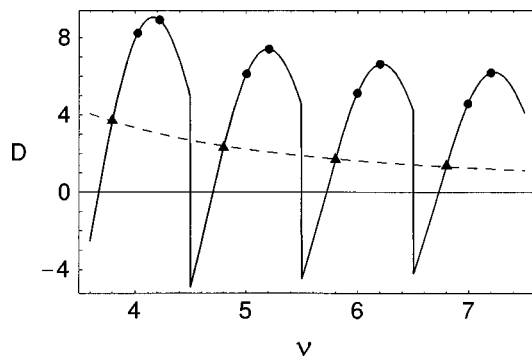


FIG. 3. $\bar{D}_C^d(R=3)$ (solid line) (in units of $a_0\mathcal{R}^{-1}$, where $\mathcal{R}$ is the Rydberg constant), plotted as a function of the effective quantum number $\nu$. Dots relate to energies of physical bound states. Triangles, connected by the dashed curve, correspond to $\varkappa=-0.2$. The discontinuities at each half-integer value of $\nu$ result from our sign convention.

$$E(R)=\epsilon+E_{1\sigma_g}^+(R). \qquad (33)$$

$\epsilon$ is then the energy of a Rydberg electron orbiting around an ion core in its ground state [from Eq. (7) we see that $\epsilon=\epsilon_d$]. The pairs of solid circles correspond to the physical bound states of the clamped-nuclei $\Sigma_g^+$ molecule. Although there are three channels involved in the $\Sigma_g^+$ states, there are no physical bound states for the excited core $p$ channel for $R=3$ in the energy range considered. Despite the fact that in this case the two closed circles within each pair are quite close to each other, their $C\rightarrow d$ channel transition moments are different. In fact, as can be seen by following the solid line, as $\nu$ increases the $C\rightarrow d$ channel transition moment undergoes a strong oscillation. On the other hand, a smooth energy variation is obtained for any constant value of $\varkappa$ (and related $\nu$ values given by $\nu=\varkappa+n'$). In Fig. 3 the triangles correspond to $\varkappa=-0.2$ and the dashed line interpolating between these points illustrates the smooth energy dependence and thus that of $d_1(\epsilon_i)$ of Eq. (20). Note that the discontinuity at each half-integer value of $\nu$ results from a global sign change. By calculating also $\bar{D}_C^s(R=3)$ and $\bar{D}_C^p(R=3)$, Eq. (16) then gives the global electronic dipole moment at the selected energy.

### 2. Parametrized transition moment

From Eq. (25) we can compute parametrized transition moments that have the main advantage of having a pure smooth energy dependence. For example, the calculation of electronic transition moments $D_B^{\Sigma_g}(R)$ from the $B$ state to high Rydberg or autoionizing $^1\Sigma_g^+$ states requires the determination of $D_B^s(R)$, $D_B^d(R)$, and $D_B^p(R)$ [see Eq. (11) or (32)]. These three components are displayed in Fig. 4 for molecular energies that cross the first ionization threshold, the energy scale $\epsilon$ being given by Eq. (33).

Notice that for each value of the internuclear distance these energy-normalized components have a smooth energy variation. They are also smooth with changing $R$, with the bump that lies between 2.5 and 4.5 a.u. being primarily due to transitions induced by electronic interactions. The bump is less obvious in $D_B^d(R)$ because $p\rightarrow d$ is the dominant transition. This overall smooth character makes parametrized transition moments well suited for use with the frame transformations described in Eqs. (26)–(29) above.

## V. DISCUSSION

### A. Validity of the Coulomb approximation

Since Bates and Damgaard's original paper, the Coulomb approximation for transitions between excited states of effective one-electron atoms has been compared to model potentials and self-consistent methods rather successfully, high accuracy being achieved when the outer electron's wave function was simply set to zero in the transition integrals [17–19]. Some problems could be expected with low Rydberg energy wave functions (for $\nu_i \lesssim l+1$) because they are rather compact: When they approach the core from outside, these low-energy functions diverge before reaching an extremum (i.e., a substantial part of the outer electron's wave function lies inside the core); the stability of the integral is
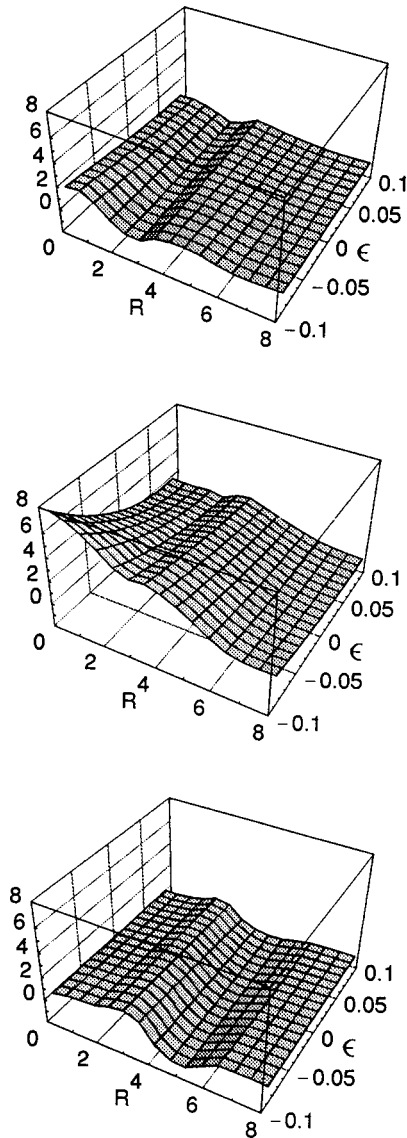
FIG. 4. From top to bottom, parametrized transition moments $D_B^s$, $D_B^d$, and $D_B^p$ (in units of $a_0 \mathcal{R}^{-1}$) plotted on an internuclear distance grid $R$ (in units of $a_0$) as functions of the electron energy relative to the $1\sigma_g$ core $\epsilon$ (in units of $\mathcal{R}$).

then by no means evident. While some authors argued that the Coulomb approximation was not valid at low energies (see, e.g., [20]) others just noticed a loss of accuracy [19]. In our $H_2$ example, low-energy ''Rydberg'' electron states are commonly encountered even for high molecular energies because of the channels built on the excited core ($p$ electron). Our good agreement with *ab initio* calculations gives us confidence in the use of the Coulomb approximation even when $\nu_i \lesssim l+1$. The situation can only get better when transitions towards more excited states are calculated.

We know that the outer electron does not have any appreciable screening effect on core transitions [21], but the transition probability is lowered because the outer electron needs to readjust to the situation (which might include an energy loss if the photon energy is smaller than the energy difference between initial and final core states). This readjustment, and consequently the core transition, is possible only if there is some appreciable overlap between the initial and final outer-electron wave functions [see the term in the second set

of curly brackets in Eq. (32)]. The reservations made for $\nu_i \lesssim l+1$ still hold in principle. However, we have seen in Figs. 1 and 2 the good agreement between the current results, where the dipole moments contain large contributions from core transitions, and the *ab initio* computations.

### B. Large internuclear distance behavior

It is known that the molecular-orbital method breaks down at large $R$ because of major configuration mixing, as Mulliken has pointed out [22]. Instead, the wave functions are more simply described as linear combinations of atomic substates in the separated atomic-orbital approximation. This is related to the fact that the core electron tends to go with one of the nuclei and the outer electron adjusts accordingly to one or the other, resulting in covalent or ionic configurations.

Notwithstanding, it is shown elsewhere [23] that the effective quantum number $\nu_i$ in each channel $i$ still has a simple significance in most of the molecular energy–$R$ coordinate plane: For $R>8$ a.u. the core electron is adequately represented as a $1s$ electron orbiting around one or the other nucleus. When the other electron adjusts, we usually get a symmetrized $H(1s)+H(\nu_i l)$ covalent configuration; $\nu_i$ is then very close to a whole number and represents a H-electron principal quantum number, the departure from a whole number giving an idea of electron-interatomic interactions. When the ionic configuration predominates, $\nu_i$ represents the binding energy of $H^-$ corrected by interatomic interactions.

Thus at large $R$, the MQDT wave functions that describe a core and an outer electron suffer from three main problems.

(i) The outer electron function remains formally centered on the internuclear midpoint.

(ii) The core electron becomes an even or odd linear combination of a $1s$ electron centered on each of the now separated nuclei, regardless of the outer electron's behavior, while in fact the outer electron should adjust as already mentioned.

(iii) Electronic channels that could be neglected at smaller $R$ (except maybe for very high energies) come into play; furthermore, we know that for large internuclear distances our quantum-defect matrix gives an incomplete physical picture since the nondiagonal quantum defects have been artificially turned off [4].

In calculating dipole transitions, the three problems just mentioned can be dealt with respectively in each of the following ways [23].

(i) The dipole transition moment for the *outer* electron calculated with the MQDT functions is equivalent to a pure covalent transition between separated atoms. Since the $C$ and $R$ states of Sec. IV B have pure covalent configurations [7], we expect our calculations for this example to be correct even at large distance, as was indeed seen to be the case in Fig. 2(b). If, on the other hand, one or both states have a ionic configuration, an extra term representing a transition between electrons on different nuclei must be added to the MQDT expression.

(ii) The dipole transition moment for the *core* electron calculated with the MQDT functions is equivalent to a transition between pure ionic configurations. Consequently, if

none of the states has ionic components, our MQDT core transition must be set to zero. This is illustrated by our calculations for the transition from $C$ to $I$ [Fig. 2(a)]. It is known that none of these states has ionic components and we thus set the core dipole moment (that is the $(1s\sigma_g)$ $\times(\epsilon_C p\pi_u)\rightarrow(2p\sigma_u)(\epsilon_I p\pi_u)$ transition) to zero gradually at large $R$. On the other hand, if only one of the functions has an ionic configuration, an extra term representing an overlap between electrons on different nuclei has to be added to the MQDT expression.

(iii) The $B$-$H\bar{H}$ transition provides an example of the incomplete channel representation of our MQDT functions. Since our main concern is the transition between $B$ and higher $\Sigma_g$ states, we are not really interested in the exact channel composition of the $H\bar{H}$ state, which we know in any case not to be adequately represented by our MQDT functions at large $R$. However, an accurate representation of the lower (here $B$) state, say by *ab initio* computations, is important if we wish to compute $B\rightarrow s$, $d$, or $p$ channel transitions. In this case a quantitative analysis of the $B$ state is available [24]. The effects of the missing channel are then accounted for by following the prescriptions of Ref. [23] outlined in the two points above.

## VI. CONCLUSION

In this work we have developed a formulation for calculating dipole moments within a collision theory framework, with the inclusion of core transitions. The validity of the Coulomb approximation in practical calculations was tested by comparison with *ab initio* results for selected transitions of $H_2$. The treatment of the energy dependence of the radial integrals may straightforwardly be extended in the case of generalized fields (i.e., not purely Coulomb outer field). The next phase of the work, namely, the computation of several ionization and dissociation spectra of $H_2$ using these transition moments, is in progress. Recent experiments [25] have shown that dipole moments at large internuclear distance cannot be neglected, particularly when states with outer minima are studied; this is why we have included in our study *ad hoc* modifications at large internuclear distance.

[1] Ch. Jungen and G. Raseev, Phys. Rev. A **57**, 2407 (1998).
[2] M. J. Seaton, J. Phys. B **14**, 3827 (1981).
[3] S. C. Ross and Ch. Jungen, Phys. Rev. A **49**, 4353 (1994).
[4] S. C. Ross and Ch. Jungen, Phys. Rev. A **49**, 4364 (1994).
[5] C. Zhu, J. G. Wang, Y. Z. Qu, and J. M. Li, Phys. Rev. A **57**, 1747 (1998).
[6] L. Wolniewicz and K. Dressler, J. Mol. Spectrosc. **96**, 195 (1982).
[7] L. Wolniewicz, J. Mol. Spectrosc. **180**, 398 (1996).
[8] M. J. Seaton, Rep. Prog. Phys. **46**, 167 (1983).
[9] C. Cornaggia, A. Giusti-Suzor, and Ch. Jungen, J. Chem. Phys. **87**, 3934 (1987).
[10] Ch. Jungen, S. T. Pratt, and S. C. Ross, J. Phys. Chem. **99**, 1700 (1995).
[11] G. Laplanche, M. Jaouen, and A. Rachman, J. Phys. B **16**, 415 (1983).
[12] A. Giusti-Suzor and U. Fano, J. Phys. B **17**, 215 (1984).

[13] J. M. Lecomte, J. Phys. B **20**, 3645 (1987).
[14] D. R. Bates and A. Damgaard, Philos. Trans. R. Soc. London, Ser. A **242**, 101 (1949).
[15] D. E. Ramaker and J. M. Peek, At. Data **5**, 167 (1973).
[16] S. C. Ross and Ch. Jungen, Phys. Rev. A **50**, 4618 (1994).
[17] C. Laughlin, Phys. Scr. **45**, 238 (1992).
[18] A. Lindgard and S. E. Nielsen, J. Phys. B **8**, 1183 (1975).
[19] A. Lindgard and S. E. Nielsen, At. Data Nucl. Data Tables **19**, 533 (1977).
[20] M. Rahman-Attia, M. Jaouen, G. Laplanche, and A. Rachman, J. Phys. B **19**, 897 (1986).
[21] U. Fano and T. Cooper, Rev. Mod. Phys. **40**, 441 (1968).
[22] R. S. Mulliken, J. Am. Chem. Soc. **88**, 1849 (1966).
[23] A. Matzkin and Ch. Jungen (unpublished).
[24] W. Kołos and L. Wolniewicz, J. Chem. Phys. **45**, 509 (1966).
[25] E. Reinhold, W. Hogervorst, and W. Ubachs, Phys. Rev. Lett. **78**, 2543 (1997).